

Dichotomy between RIP1- and RIP3-Mediated Necroptosis in Tumor Necrosis Factor- α -Induced Shock

Andreas Linkermann,¹ Jan H Bräsen,² Federica De Zen,¹ Ricardo Weinlich,³ Reto A Schwendener,⁴ Douglas R Green,³ Ulrich Kunzendorf,¹ and Stefan Krautwald¹

¹Division of Nephrology and Hypertension, Christian-Albrechts University, Kiel, Germany; ²Division of Pathology, Christian-Albrechts University, Kiel, Germany; ³Department of Immunology, St. Jude Children's Research Hospital, Memphis, Tennessee, United States of America; and ⁴Institute of Molecular Cancer Research, University of Zurich, Switzerland

Tumor necrosis factor receptor (TNFR) signaling may result in survival, apoptosis or programmed necrosis. The latter is called necroptosis if the receptor-interacting protein 1 (RIP1) inhibitor necrostatin-1 (Nec-1) or genetic knockout of RIP3 prevents it. In the lethal mouse model of TNF α -mediated shock, addition of the pan-caspase inhibitor zVAD-fmk (zVAD) accelerates time to death. Here, we demonstrate that RIP3-deficient mice are protected markedly from TNF α -mediated shock in the presence and absence of caspase inhibition. We further show that the fusion protein TAT-crmA, previously demonstrated to inhibit apoptosis, also prevents necroptosis in L929, HT29 and FADD-deficient Jurkat cells. In contrast to RIP3-deficient mice, blocking necroptosis by Nec-1 or TAT-crmA did not protect from TNF α /zVAD-mediated shock, but further accelerated time to death. Even in the absence of caspase inhibition, Nec-1 application led to similar kinetics. Depletion of macrophages, natural killer (NK) cells, granulocytes or genetic deficiency for T lymphocytes did not influence this model. Because RIP3-deficient mice are known to be protected from cerulein-induced pancreatitis (CIP), we applied Nec-1 and TAT-crmA in this model and demonstrated the deterioration of pancreatic damage upon addition of these substances. These data highlight the importance of separating genetic RIP3 deficiency from RIP1 inhibition by Nec-1 application *in vivo* and challenge the current definition of necroptosis.

Online address: <http://www.molmed.org>

doi: 10.2119/molmed.2011.00423

INTRODUCTION

Programmed cell death (PCD) was used synonymously with caspase-dependent apoptosis until caspase-independent cell death pathways were discovered (1–4). PCD undoubtedly is of outstanding clinical interest (5,6). In tumor necrosis factor receptor (TNFR) signaling, the conglomerate of TNFR, TNFR1-associated DEATH domain protein (TRADD), TNFR-associated factor 2 (TRAF2), polyubiquitylated RIP1 and inhibitor of apoptosis proteins (IAPs), called complex I, results in nuclear factor- κ B (NF- κ B)-mediated pro-survival signaling. Recently, the linear

ubiquitin chain assembly complex (LUBAC) has been demonstrated not only to be an important part of complex I, but also to be an important regulator of proinflammatory cell death induction by TNF (7,8). The capability of cells to undergo PCD following TNFR ligation depends on deubiquitylation of RIP1, causing changes in complex I composition (9,10) which switches off the NF- κ B pathways and enables PCD signaling via complex II. PCD encompasses both apoptosis and programmed necrosis, which signal via complex IIa and complex IIb, respectively (10–13). Complex IIa involves activation

of a caspase-8/FLIP_L heterodimer that leads to RIP1 inactivation, thereby preventing the assembly of complex IIb (14). In the absence of caspase-8, or if the heterodimer is blocked (for example, by caspase inhibitors), RIP1 is not inactivated and complex IIb mediates TNF-mediated programmed necrosis (PN).

RIP1- and/or RIP3-dependent PN has been defined recently as necroptosis in the presence of caspase inhibition (15). In the case of TNFR ligation, necroptotic cell death was demonstrated in various cell lines (for example, L929, HT29 and FAS-associated death domain protein (FADD)-deficient Jurkat cells) (12,16,17). *In vivo*, infection with vaccinia virus led to 100% lethality of RIP3-deficient mice whereas wild-type mice survived this infection (18). Consequently, necroptosis has been interpreted as a mechanism of host defense against caspase inhibitor-expressing viruses (11,18). Further, physiologically relevant necroptosis has been demonstrated in T lymphocytes (19),

Address correspondence to Ulrich Kunzendorf, Christian-Albrechts University Kiel, Division of Nephrology and Hypertension, Schittenhelmstr. 12, 24105 Kiel, Germany. Phone: +49-431-597-1336; Fax: +49-431-597-1337; E-mail: kunzendorf@nephro.uni-kiel.de.

Submitted November 2, 2011; Accepted for publication February 17, 2012; Epub (www.molmed.org) ahead of print February 24, 2012.

photoreceptors (20) and in a stroke model (21), and has been suggested to contribute to the pathogenesis of myocardial infarction (22) and kidney ischemia/reperfusion injury (23). Additional evidence for the *in vivo* relevance of RIP3 has been added recently by the fact that this protein mediates the lethal phenotype of caspase-8 deficient mice (14,24). Above that, RIP3 deficiency partially protects from cerulein-induced pancreatitis (CIP), suggesting that necrotizing pancreatitis may be attenuated by pharmacological interference of this pathway (16,25). The extraordinary specificity of Nec-1 to interfere with RIP1 phosphorylation has been studied extensively (26,27) and has been demonstrated to protect from myocardial infarction and stroke *in vivo* (21,22). Because attempts to block apoptosis in lethal TNF α -mediated shock employing the pan-caspase inhibitor zVAD-fmk (zVAD) resulted in hyperacute TNF α /zVAD-mediated shock and accelerated the time to death (28), necroptosis has been discussed to contribute to this model (27). Finally, under certain circumstances, RIP1- and RIP3-independent programmed necrosis has been demonstrated (29,30).

To inhibit PCD, we generated a protein that consists of HIV TAT fused to the cowpox virus protein crmA (31), and showed that TAT-crmA efficiently blocks Fas-mediated apoptosis (32). Here, we demonstrate that TAT-crmA effectively blocks necroptosis in L929, HT29 and in FADD-deficient Jurkat cells and that RIP3-deficient mice are protected from acute TNF α -mediated and hyperacute TNF α -zVAD-mediated shock. Consequently, we aimed to improve *in vivo* necroptosis models by Nec-1 and TAT-crmA. Unexpectedly, we found that neither drug protected the mice, but rather accelerated the time to death after TNF α -mediated shock, TNF α /zVAD-mediated hyperacute shock and deteriorated cerulein-induced pancreatitis (CIP). Above that, Nec-1 by itself worsened the outcome of these models independent of caspase inhibition. These data highlight that genetic RIP3-deficiency and RIP1 in-

hibition by Nec-1 application need to be separated carefully.

MATERIALS AND METHODS

Reagents and Antibodies

The zVAD, the ApoAlert annexin V-FITC antibody α -FADD, α -RIP1 and the monoclonal α -crmA antibody were purchased from BD Biosciences (Heidelberg, Germany). Recombinant mouse TNF α (carrier-free) and purified α -human TNF α were purchased from BioLegend (Uithoorn, Netherlands). The cyclophilin A antibody and the caspase-8 antibody were obtained from Cell Signaling (Frankfurt/Main, Germany). The reagents cycloheximide (CHX), necrostatin-1 (Nec-1) and cerulein were obtained from Sigma-Aldrich (Taufkirchen, Germany).

Cell Culture

Jurkat cells, HT29 adenocarcinoma cells and L929 fibrosarcoma cells were originally obtained from ATCC (Manassas, VA, USA). FADD-deficient Jurkat cells were kindly provided by Dieter Adam (Institute for Immunology, UK-SH Kiel, Germany). Parental and FADD-deficient Jurkat cells were cultured in RPMI medium supplemented with 10% fetal calf serum (FCS) and penicillin-streptomycin. HT29 cells were maintained in minimum essential medium with Earle's salts (Invitrogen, Darmstadt, Germany), 10% FCS with glutamine, penicillin-streptomycin, nonessential amino acids and sodium pyruvate. L929 cells were cultured in Dulbecco's modified Eagle medium (DMEM) (Invitrogen) supplemented with 10% FCS and penicillin-streptomycin. All cell lines were cultured in a humidified 5% CO₂ atmosphere.

Cloning, Expression and Purification of Recombinant Proteins

Bacterial expression and purification of recombinant TAT-crmA and mutated TAT-crmA (mut.TAT-crmA) fusion proteins were modified slightly from the previously described procedure (32) and

are described in detail in Supplemental Information.

Assessment of Cell Death

Phosphatidylserine exposure to the outer cell membrane was quantified by annexin V staining followed by fluorescence-activated cell sorting (FACS) analysis. Cells were stimulated for 5 h at 37°C with 100 ng/mL TNF α , 2 μ g/mL CHX, 30 μ mol/L Nec-1, 25 μ mol/L zVAD or 500 nmol/L TAT-crmA as indicated. Annexin V-staining was performed according to the manufacturer's instructions. Fluorescence was analyzed using an EPICS XL (Beckman Coulter, Krefeld, Germany) flow cytometer. Data were analyzed using EPICS System II software. The biomarker cyclophilin A is released from necroptotic cells. For this, L929 cells were treated for 7 h at 37°C with the indicated reagents. The supernatants (200 μ L) were isolated and analyzed by SDS-PAGE followed by Western blotting using α -CypA antibody, as published previously (33).

Animals and *In Vivo* Models

Six- to eight-week old female C57BL/6 mice (average weight approximately 22 g) and 6- to 8-wk old female Balb/c mice (average weight approximately 20 g) were purchased from Charles River (Sulzfeld, Germany). Female mice were used in all experiments unless otherwise specified. RIP3-deficient mice were described previously (14) and were obtained initially from VM Dixit (34). All mice were kept on a standard diet and a 12 h day-night rhythm. All *in vivo* experiments were performed according to the *Protection of Animals Act* after approval. In all experiments, mice were carefully matched for age, sex, weight and genetic background.

The model of TNF α -induced shock has been described in detail previously (28). In our experiments, C57BL/6 mice or Balb/c mice received intraperitoneal (i.p.) injections (total volume per mouse was 200 μ L) of either vehicle, 10 mg zVAD/kg body weight, 1.65 mg Nec-1/kg body weight, 20 mg TAT-crmA/kg body weight,

20 mg mut.TAT-crmA/kg body weight or combined reagents as indicated 15 min prior and 1 h after singular injection of 25 μ g murine TNF α in 200 μ L PBS via the tail vein in the identical concentration, respectively, with the exception of zVAD, of which 2 mg/kg body weight was applied at the time of the second injection. Animals were under permanent observation and survival was checked every 15 min. In an analogous experiment, all animals (n = 3 per group) were euthanized 3 h after TNF α injection and tissue samples were harvested and transferred to 4% normal-buffered formalin for histological preparation.

Cerulein-induced pancreatitis (CIP) has been described elsewhere in detail (16). Briefly, C57BL/6 mice received i.p. injections of 50 μ g cerulein/kg body weight once every h for 10 h. Equal volumes (150 μ L) of vehicle, 10 mg zVAD/kg body weight, 1.65 mg Nec-1/kg body weight or 10 mg TAT-crmA/kg body weight were injected i.p. 10 min before cerulein injection. Every 2 h later for 10 h in total, one fifth of the above mentioned concentration was applied in equal volumes. Animals were euthanized 24 h after the first injection and samples of blood and tissues were rapidly harvested. Quantification of pancreas injury was performed by measuring serum amylase and lipase activity. Whole pancreas organs were excised and transferred to 4% normal-buffered formalin for histological preparation. Overall pancreatic damage scores were calculated by a pathologist using a scale from 0 to 5 with consideration of these independent parameters: edema formation, immune cell infiltration, tissue necrosis and structural organ conservation.

Histology and Immunohistochemistry

Organs were recovered as indicated and fixated with 4% neutral-buffered formalin paraffin-embedded. Samples were sectioned and stained with hematoxylin–eosin (HE) or periodic acid–Schiff (PAS) reagent, respectively, according to routine protocols and ex-

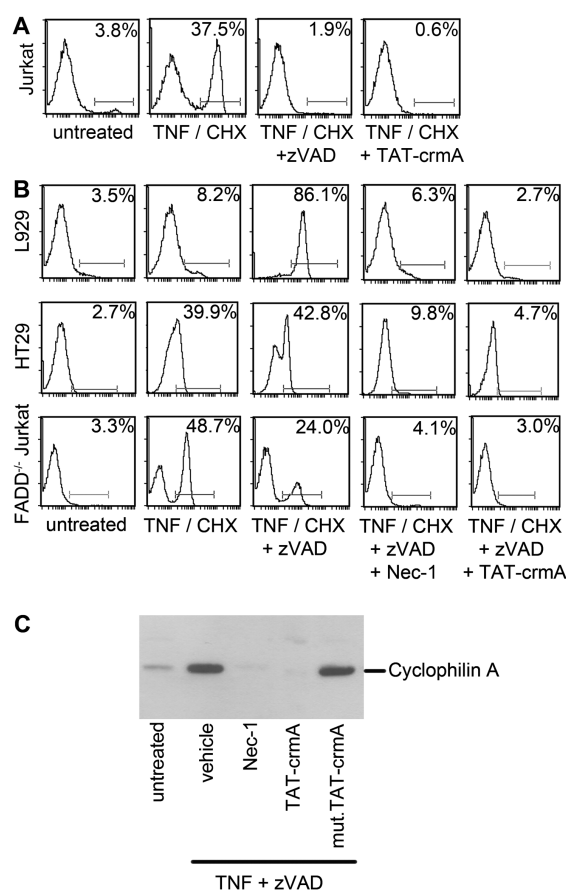


Figure 1. TAT-crmA inhibits both apoptosis and necroptosis *in vitro*. (A) Jurkat T cells were left untreated or treated with recombinant human TNF α plus CHX, zVAD and TAT-crmA as indicated. After 5 h of incubation at 37°C, cells were stained for phosphatidylserine exposure with annexin V-FITC antibody and analyzed by FACS. Presence of zVAD or TAT-crmA prevented TNF α /CHX-induced apoptotic cell death. (B) L929, HT29 and FADD^{-/-} Jurkat cells were left untreated or treated with TNF α plus CHX, zVAD, Nec-1 and TAT-crmA as indicated. After 5 h of incubation at 37°C, cells were stained with annexin V-FITC and analyzed by FACS. Necroptosis was induced by TNF α /CHX + zVAD and protection from necroptotic cell death was achieved by the addition of Nec-1 or TAT-crmA. (C) Western blot of cyclophilin A in the supernatant of L929 cells that were left untreated or treated for 7 h with TNF α , zVAD, Nec-1, TAT-crmA or mut.TAT-crmA, as indicated.

amined for pathological changes under an Axio Imager microscope (Zeiss, Oberkochen, Germany) at 200 \times (pancreas and jejunum) or 400 \times (kidney) magnification. High-resolution imaging was documented using an AxioCam MRm Rev. 3 FireWire camera and AxioVision Rel. 4.5 software (Zeiss, Germany). Organ damage (kidney and pancreas) was quantified by a pathologist in a double-blind manner on a scale ranging from 0 (unaffected tissue) to 10 (severe organ damage).

Statistics

Differences in compared groups were considered statistically significantly different with *P* values lower than 0.05 and were marked with * as calculated with student *t* tests. Highly significant differences were indicated with ** when *P* < 0.01 and *** when *P* < 0.001. Calculation of *t* tests was performed using the GraphPad Prism software, version 5.04.

All supplementary materials are available online at www.molmed.org.

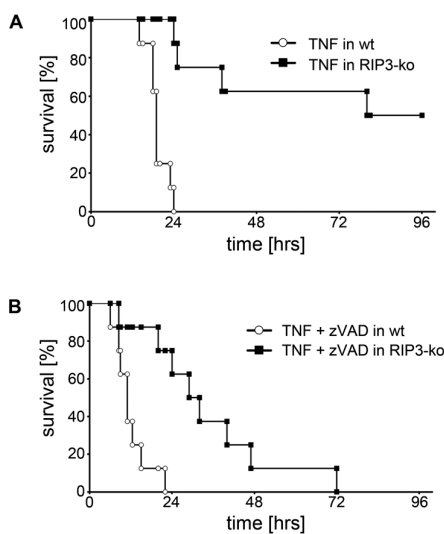


Figure 2. Genetic deficiency of RIP3 protects from TNF α -mediated shock in the presence and absence of caspase inhibition. Wild-type mice (open circles) and RIP3-deficient mice (black squares, $n = 8$ per group) were treated with mouse TNF α in the absence (A) or presence (B) of zVAD. Survival is presented as a Kaplan-Meier plot. Genetic RIP3-deficiency protects from both TNF α -mediated shock ($P < 0.001$) and hyperacute TNF α /zVAD-mediated shock ($P < 0.01$), respectively.

RESULTS

TAT-crmA Inhibits TNF α -Mediated Apoptosis

To induce caspase-dependent TNFR-mediated extrinsic apoptosis, Jurkat cells were treated with 100 ng/mL recombinant human TNF α plus 2 μ g/mL cycloheximide (CHX), 25 μ mol/L of the pan-caspase inhibitor zVAD and 500 nmol/L TAT-crmA as indicated. After 5 h of incubation at 37°C, cells were stained for phosphatidylserine exposure with annexin V-FITC and analyzed by flow cytometry (FACS). The presence of zVAD or TAT-crmA completely prevented TNF α /CHX-induced apoptotic cell death (Figure 1A). In this context, we demonstrated previously that TAT-crmA promotes a significant reduction of ischemic myocardial tissue injury (32). Because of the latter observation and a recent publication that ascribes a pathophysiological

impact to both apoptosis and programmed necrosis in myocardial infarction (35), we hypothesized that TAT-crmA, besides blocking apoptosis, also might interfere with the necroptosis pathway.

TAT-crmA Inhibits TNF α -Mediated Necroptosis

To investigate the potential of TAT-crmA to prevent TNF α -mediated programmed necrosis, L929, HT29 and FADD-deficient Jurkat cells, were incubated for 5 h at 37°C with 100 ng/mL recombinant TNF α plus 2 μ g/mL CHX in the presence or absence of 25 μ mol/L zVAD, 30 μ mol/L of Nec-1 or 500 nmol/L TAT-crmA. Accessibility to phosphatidylserine residues was analyzed by FACS staining using an annexin V-FITC antibody. This readout was demonstrated previously to be appropriate for evaluation of necroptosis in the presence of Nec-1 (36). As shown in Figure 1B, the percentage of necroptotic cells induced by TNF α /CHX in combination with zVAD was significantly reduced by the addition of Nec-1 or TAT-crmA. In FADD-deficient Jurkat cells, the presence of two independent cell death pathways was obvious. Blocking TNF α /CHX-induced apoptosis with zVAD reduced the number of annexin V-positive cells from 48.7% to 24.0%. The existing fraction of necroptotic cells was rescued to basal levels by the addition of Nec-1 or TAT-crmA. TAT-crmA was at least as effective as Nec-1 in reducing cell death in all three investigated cell lines. To confirm this result in an independent second readout system, we investigated cyclophilin A release which was suggested as a marker for necrotic cell death (33). To assess cyclophilin A release, L929 cells were left untreated or treated with 100 ng/mL TNF α + 25 μ mol/L zVAD (TZ), TZ + 30 μ mol/L Nec-1, TZ + 500 nmol/L TAT-crmA, and TZ + 500 nmol/L of an inactive mutant of TAT-crmA (mut.TAT-crmA), respectively, as indicated for 7 h at 37°C. Supernatants were harvested and Western blotting was performed using a cyclophilin A antibody

(Figure 1C). Blockade of necroptosis with either Nec-1 or TAT-crmA reduced the amount of cyclophilin A to basal levels in an equally effective manner whereas the mut.TAT-crmA did not prevent cyclophilin A release. Because of the endogenous TNF α -production of L929 cells (33,37), we additionally assessed cyclophilin A release in the absence of exogenously added TNF α . As demonstrated in Figure S1, both Nec-1 and TAT-crmA reduced the amount of cyclophilin A released into the supernatant.

To get mechanistic insights into how the fusion protein TAT-crmA interferes with the necroptotic signaling complexes, we analyzed lysates from RIP3-overexpressing cells for a possible interaction with TAT-crmA. As demonstrated in Figure S2A, TAT-crmA but not mut.TAT-crmA immunoprecipitated RIP3. Under identical conditions, no immunoprecipitation of RIP1, FADD or caspase-8 was detected (Figure S2B).

RIP3-Deficient Mice Are Protected from TNF α -Mediated Shock and TNF α /zVAD-Mediated Hyperacute Shock

In search for a suitable model of necroptosis to transfer our *in vitro* data into an *in vivo* setting, we evaluated the well-established mouse models of acute TNF α -induced and hyperacute TNF α /zVAD-mediated shock. In the latter, caspase-blockade with zVAD combined with intravenous (i.v.) application of TNF α leads to accelerated death in wild-type mice (28). Because mice deficient in RIP1, the direct target of Nec-1, fail to thrive and die at d 1 to 3 after birth, we investigated mice that are genetically deficient for RIP3, an essential component of the necroptosome. The functional relevance of RIP3 was assessed in both TNF α -mediated acute and TNF α /zVAD-mediated hyperacute shock as induced by treatment with i.v. injection of 25 μ g murine TNF α alone (Figure 2A, $n = 8$) or a combination of TNF α and 250 μ g zVAD. The latter was injected i.p. 15 min before TNF α application (Figure 2B, $n = 8$) as described in Material and Methods.

RIP3-deficient mice were significantly protected from both TNF α -induced and TNF α /zVAD-mediated hyperacute shock ($P = 0.0013$ and $P < 0.0001$, respectively). In the TNF α -induced shock model, 50% of RIP3-deficient mice survived the experiment whereas only one RIP3-knockout (ko) mouse survived the TNF α /zVAD-mediated hyperacute shock, respectively. All wild-type mice died within 24 h after TNF α -injection. In a similar experiment, male wild-type mice were compared with male RIP3-ko mice in the TNF α -shock model with comparable results (data not shown). Interestingly, the RIP3 pathway appears to be involved in the TNF α model wherein it does not require pharmacological caspase inhibition. These data highlight that necroptosis by definition contributes to both of these processes.

The Necroptosis Blockers Nec-1 and TAT-crmA Accelerate Time to Death after Hyperacute TNF α /zVAD-Induced Shock

Given that both Nec-1 and TAT-crmA are potent blockers of necroptosis *in vitro* (Figure 1) and the relevance of RIP3-dependent necroptosis in the TNF α /zVAD-mediated hyperacute shock model (see Figure 2B), we aimed to apply Nec-1 and TAT-crmA in this model. Mice ($n = 7$) died after 24.43 ± 3.64 h when treated with TNF α alone and the addition of zVAD led to a significantly shorter time to death (13.50 ± 6.25 h, $P < 0.001$) (Figure 3A). However, one mouse survived the experiment. This finding is consistent with previously published data (28). Consequently, we aimed to prolong survival by adding Nec-1 or TAT-crmA. To this end, TNF α /zVAD-treated mice received two i.p. injections of 1.65 mg Nec-1/kg body weight or 20 mg TAT-crmA/kg body weight. The first was given 15 min before, the second, 1 h after application of TNF α . Surprisingly, mice in both groups died significantly earlier than the TNF α /zVAD-treated mice (TNF α /zVAD/Nec-1-treated and TNF α /zVAD/TAT-crmA-treated mice died after 7.14 ± 3.44 h [$P < 0.05$] and 9.14 ± 3.24 h [$P < 0.05$], respectively). In a

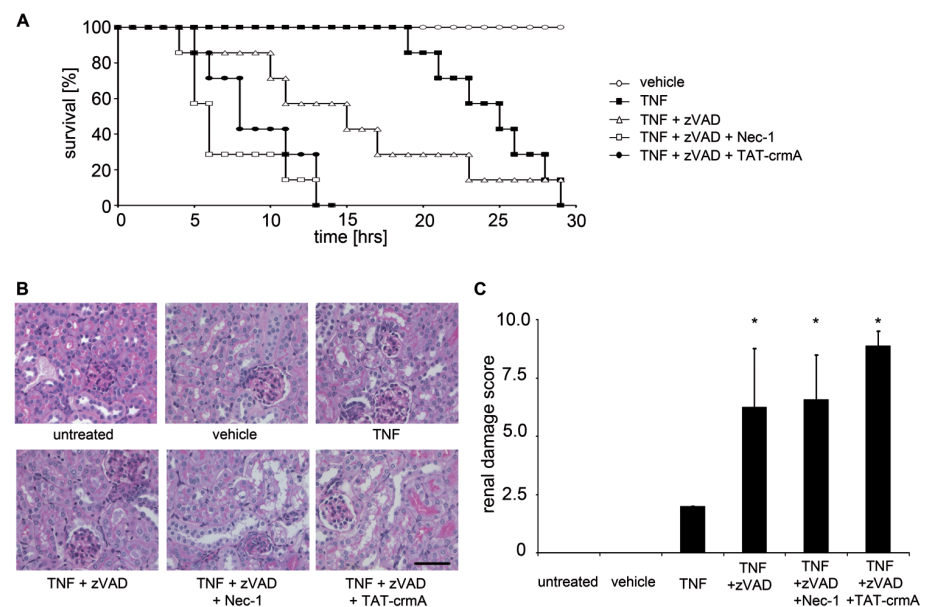


Figure 3. Blocking necroptosis accelerates death and worsens organ damage after TNF α /zVAD-mediated hyperacute shock. (A) Mice were left untreated (open circles), injected intravenously with mouse TNF α alone (black squares) or in addition with zVAD (open triangles), zVAD + Nec-1 (open squares) or zVAD + TAT-crmA (black circles). Survival is presented as a Kaplan-Meier plot. Whereas TNF α -treated mice die significantly later than TNF α /zVAD-treated animals ($P < 0.01$), both TNF α /zVAD/Nec-1- and TNF α /zVAD/TAT-crmA-treated mice died significantly earlier compared with TNF α /zVAD-treated mice ($P < 0.02$, $n = 7$). (B) Three h after TNF α -injection (basic experimental setting is identical to 3A), mice were euthanized, and kidneys were harvested and prepared for PAS-staining. Representative sections are shown, and a renal damage score was used for quantification. (C) Compared to the TNF α -treated group, significantly elevated renal damage was detected in the TNF α /zVAD-, TNF α /zVAD/Nec-1- and the TNF α /zVAD/TAT-crmA-treated animals ($n = 3$). Scale bar, 20 μ m.

separate experiment, we induced hyperacute TNF α /zVAD-mediated shock in identical settings and euthanized the mice 3 h after TNF α injection and harvested organs (heart, lungs, liver, kidneys, spleen, thymus and brain). In line with previously published data (28), the most pronounced organ damage was observed in the kidneys. Histopathological PAS staining and renal damage scores are depicted in Figures 3B and 3C, respectively. Renal tubular damage was evaluated as published previously (38). Tubular damage scores were low in the TNF α -treated group. However, significant organ damage developed upon the addition of zVAD. The most severe damage was observed in kidneys from mice in which necroptosis was inhibited by Nec-1 or TAT-crmA, although no statisti-

cally significant difference was observed between the TNF α /zVAD-treated, the TNF α /zVAD/Nec-1-treated and the TNF α /zVAD/TAT-crmA-treated groups due to high standard deviation (see Figure 3C). No differences in organ architecture were detected either macroscopically or in tissue sections of the liver, lung, pancreas or spleen (data not shown). Importantly, mice treated with mut.TAT-crmA did not show any differences in survival in this setting (Figure S3). None of the mice that received identical doses of Nec-1, zVAD, or TAT-crmA without TNF α died over a period of three months (data not shown). These results suggest a deteriorating role for Nec-1 or TAT-crmA during hyperacute TNF α /zVAD-mediated shock in yet undefined cells.

Neither Genetic T-cell Deficiency in Balb/c nu/nu Mice nor Depletion of Macrophages, NK Cells or Granulocytes in Balb/c Mice Significantly Protect from Rapid Death after TNF α /zVAD/Nec-1-Mediated Hyperacute Shock

Given the aforementioned results, we hypothesized that blocking apoptosis or necroptosis by Nec-1 or TAT-crmA might rescue immune cells that might accelerate the pathogenesis of the apparent shock and harm the general organism. We targeted T lymphocytes, macrophages, natural killer (NK) cells and granulocytes as candidate cells. To relate the harmful effect to a defined immune cell population, we depleted macrophages, NK cells and granulocytes in Balb/c mice employing clodronate, monoclonal antibodies or antisera, as described in Material and Methods. Initially, successful depletion of each cell type in mice ($n = 3$) was confirmed by FACS staining in a separate approach 24 h after i.p. application of the depleting reagents (Figure S4A–C). Based on these data, we injected TNF α alone or the TNF α /zVAD/Nec-1 (TZN) after depletion and added genetically deficient nude mice (nu/nu) to the experiment. As shown in the Kaplan-Meier graph in Figure S4D, no benefit to overall survival of TNF α /zVAD/Nec-1-treated wild type mice was detected in any of the investigated transgenic or depletion mouse models ($n = 6$ in each group, TNF α data were adopted from the experiment shown in Figure 3A for better comparability). Administration of liposomes (clodronate carrier) alone did not influence survival (data not shown).

Necrostatin-1 Accelerates Time to Death and Worsens Organ Damage after TNF α -Mediated Shock in the Absence of Caspase Inhibition

Given that RIP3-deficient mice are protected not only from TNF α /zVAD-mediated hyperacute shock, but also from TNF α -induced shock (Figure 2), we investigated whether a direct blockade of RIP1 by Nec-1 might influence survival

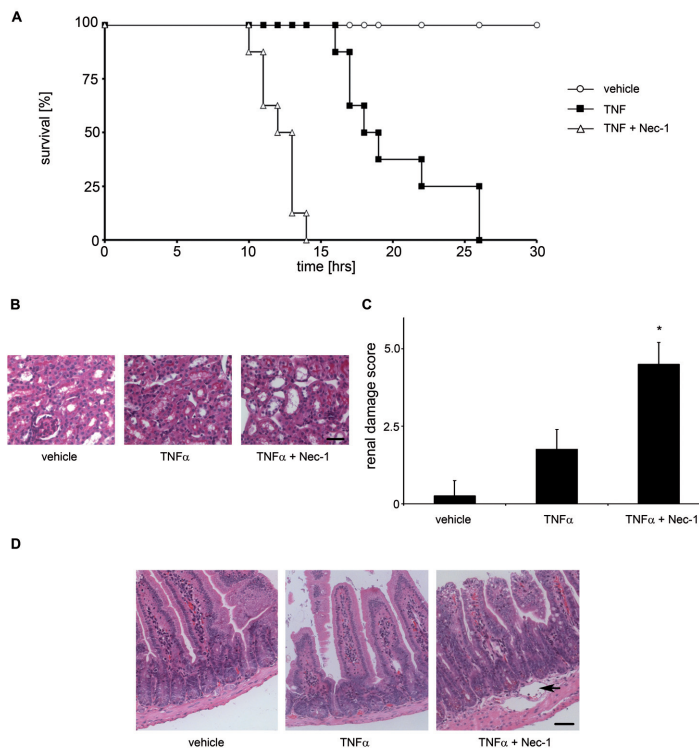


Figure 4. Necrostatin-1 accelerates death and worsens organ damage after TNF α -mediated shock in the absence of caspase inhibition. (A) Mice were left untreated (open circles) or treated intravenously with mouse TNF α alone (black squares) or in addition to Nec-1 (open triangles). Survival is presented as a Kaplan-Meier plot ($n = 8$). (B, C) Three h after TNF α -injection (basic experimental setting is identical to Figure 3A), mice were euthanized and kidneys were harvested and prepared for PAS-staining. Representative sections are demonstrated and a kidney damage score was used for quantification. (D) In an independent approach (basic experimental setting is identical to Figure 3A), 2.5 h after TNF α -injection, mice were euthanized and jejunum was harvested and HE stained. Representative sections are presented. The arrowhead points to the typical appearance of edema within the tunica muscularis that was exclusively visible in the TNF α /zVAD/Nec-1 group. Scale bars, 20 μ m (B) and 50 μ m (D).

in the TNF α -induced shock model without caspase inhibition. Interestingly, i.p. injections of Nec-1 hastened death after TNF α -induced shock in the absence of caspase inhibition. All TNF α /Nec-1-treated animals died significantly earlier compared with the TNF α -treated mice ($P < 0.001$; $n = 8$ per group, Figure 4A). Renal damage (Figures 4B, C) was increased significantly by applications of Nec-1 when compared with mice that received TNF α alone. Edema formation is indicative of the severe vascular leakage syndrome (VLS) that develops mainly in the gastrointestinal tract upon TNF α application. Consequently, we investigated

TNF α -induced gastrointestinal edema formation for each group in another independent experiment. Therefore, mice were euthanized after 2.5 h and jejunum was isolated and prepared for HE staining. Representative micrographs are shown in Figure 4D. A marked increase in gastrointestinal edema formation was obvious in the TNF α /Nec-1 group when compared with the vehicle-treated or the TNF α -treated group. Importantly, an inactive necrostatin-1 (Nec-1i) did not influence survival in this setting (Figure S5). The dose of 25 μ g TNF α per mouse was lethal in 100% of mice (see Figures 2, 3A, 4A). To further study the

deteriorating effect of Nec-1 in TNF α -mediated shock, we investigated approximately 50% lethal dose (LD₅₀) of TNF α for shock induction which was achieved by i.v. application of 9 μ g TNF α per mouse in a separate experiment. In this setting, all TNF α /Nec-1-treated mice died within 23 h whereas three of five TNF α -treated mice survived. (Figure S6, $P < 0.05$, $n = 5$ per group).

Given the presented discrepancy between RIP3-deficient mice on the one hand and necroptosis-blockers Nec-1 and TAT-crmA on the other hand, and the fact that RIP3-deficient mice are protected from cerulein-induced pancreatitis (CIP), we further investigated whether Nec-1 or TAT-crmA might exert protective or deteriorating effects in the CIP-model.

Blocking Apoptosis and Necroptosis Exacerbates Experimental Pancreatitis

Data from two independent groups demonstrated that RIP3-deficient mice were partially protected from organ damage in a model of cerulein-induced pancreatitis (CIP) (16,25). We therefore analyzed the amount of pancreatic injury upon blockade of necroptosis with Nec-1 or TAT-crmA. CIP was induced using a standard protocol (16). Administration of zVAD, Nec-1, TAT-crmA and the combination of zVAD and Nec-1 resulted in a significant increase in the serum concentrations of both amylase and lipase 24 h after the first cerulein injection (Figures 5A, B). In comparison to zVAD or Nec-1 administered alone, combined zVAD/Nec-1 or TAT-crmA treatment led to significantly higher elevation of these parameters, suggesting an additive deteriorating effect of zVAD and Nec-1. In a similar experiment, 24 h after the first cerulein injection, a double-blind evaluation of HE-stained histomicrographs revealed a marked increase in pancreatic damage scores upon treatment with TAT-crmA or a combination of zVAD and Nec-1, whereas the single components zVAD and Nec-1 did not lead to increased organ damage when compared

with vehicle-treated mice (Figures 5C, D). The reagents zVAD, Nec-1 or TAT-crmA alone, without cerulein, exhibited no effects on serum concentrations of amylase and lipase (data not shown). In identical settings, mice were observed for 8 wk after CIP-induction to exclude lethality. In this experiment, serum parameters returned to basal levels by the end of the first week (data not shown, $n = 5$). RIP3 deficient mice have been investigated in this setting previously by two other groups (16,25). Unlike Nec-1, and as expected from the above presented results concerning the TNF α -mediated shock model, RIP3-deficiency did not deteriorate the course of experimental pancreatitis in our study (data not shown). These experiments suggest an additive deteriorating effect of both zVAD and Nec-1 in CIP that appears to be reproduced by the application of TAT-crmA and demonstrate the dichotomy between RIP1- and RIP3-mediated necroptosis in a second, independent setting.

DISCUSSION

The crucial role of apoptosis in the control of certain viral infections becomes obvious with the number of virally expressed apoptosis inhibitors that target caspases (29,39–41). Viruses are easily cleared from the host organism if they are unable to respond to extrinsic apoptosis, mediated by the Fas signaling pathway (9). Among the range of viral apoptosis inhibitors, the cowpox virus protein crmA has been of outstanding interest because of its high affinity to the initiator caspase-8 (31). It is comprehensible that under evolutionary pressure, additional host defense mechanisms have emerged, including necroptosis for the rapid removal of virally infected cells that are unresponsive to conventional apoptotic signals (11,18). Interestingly, crmA efficiently blocks the caspase-8 homodimer that is responsible for the execution of apoptosis, whereas the caspase-8/FLIP_L heterodimer, which executes non-apoptotic functions, especially RIP1 inactivation, is affected by crmA only in higher doses (14).

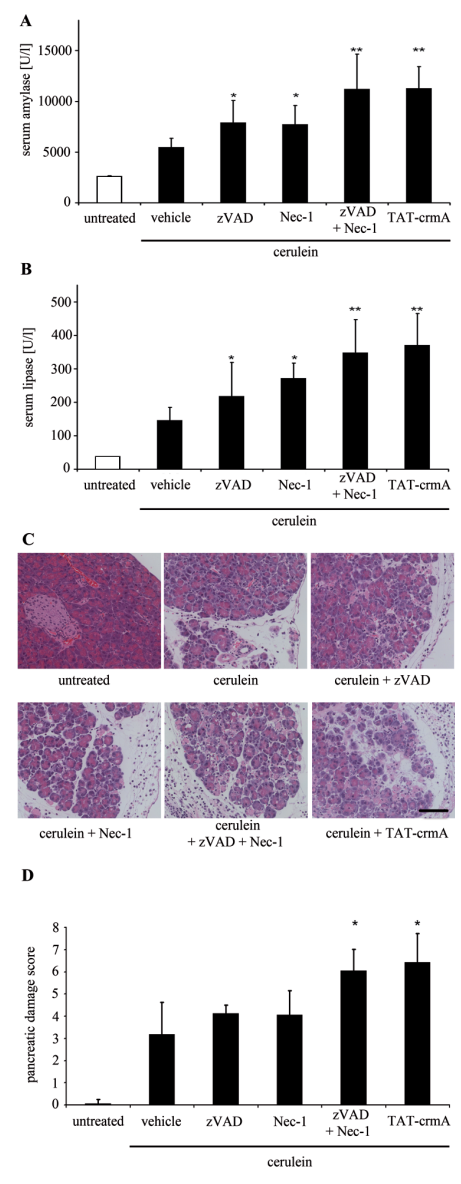


Figure 5. Blocking necroptosis deteriorates acute experimental pancreatitis. Cerulein-induced pancreatitis mice were left untreated or given i.p. injections of cerulein once every hour for 10 h. In addition to every second injection of cerulein, either vehicle or zVAD, Nec-1 and TAT-crmA were injected as indicated. 14 h after the last injection mice were sacrificed and blood samples were taken. Levels of serum amylase (A) and serum lipase (B) are shown for each group as indicated. In parallel, pancreatic tissue samples were harvested. Representative sections are demonstrated in C, and a pancreatic damage score was used for quantification (D) ($n = 5$, * $P < 0.05$, ** $P < 0.02$). Scale bar, 50 μ m.

Apoptosis has been demonstrated to be involved pathophysiologically in diverse diseases and targeting caspases has proven to be of therapeutic interest (32,42). Concerning PN cascades, evidence is accumulating that the RIP1 inhibition by Nec-1 also is of therapeutic value (21,22). Additionally, PN has been shown to be of importance in myocardial infarction and renal ischemia-reperfusion injury (23,35,43), although the interconnectivity of these pathways remains to be determined. We speculated that PCD pathways that may have emerged to defend microbes turn against the organism in ischemic, toxic or septic emergency situations (6). This hypothesis gave rise to our approach to interfering with PCD pathways by providing a viral PCD inhibitor, a directly active protein, into the vasculature of the involved organs. Importantly, the TAT-domain of HIV assures the delivery of the attached crmA into all somatic cells and can cross through the blood brain barrier (our unpublished observation). Unaware of the number of signaling pathways with which TAT-crmA interferes, we initially aimed to inhibit apoptosis in the murine model of myocardial infarction and demonstrated a noticeable protective effect (32). Moreover, others have demonstrated the pathophysiological importance of PN in myocardial infarction (35), and this prompted us to investigate the direct influence of TAT-crmA on PN. Indeed, the fusion protein inhibits necroptotic signaling (see Figure 1), whereas crmA overexpression does not (4). This discrepancy remains unexplained. We cannot exclude the possibility that the TAT-domain, perhaps guided toward the DISC by the high affinity of crmA to caspase-8, interferes with the frail assembly of complex IIa and/or complex IIb. Another possible explanation arises from the recently published observation that crmA strongly inhibits the caspase-8 homodimer which leads to cell death, but leaves the RIP1-deactivating caspase-8/FLIP_L heterodimer almost unaffected in physiological concentrations (14). Upon overexpression, crmA concentrations

might reach a level where the heterodimer also is completely blocked, thereby opening the gates for execution of necroptosis. However, TAT-crmA blocks both extrinsic apoptosis and necroptosis, comparable to the combination of zVAD and Nec-1, and additionally inhibits the intrinsic pathway (32). Those data led us to investigate the well-established model of TNF α /zVAD-induced hyperacute shock. As expected, RIP3-deficient mice are protected from TNF α /zVAD-mediated hyperacute shock. Consequently, we aimed to overcome the previously published deteriorating effect of zVAD (28) by addition of necroptosis blockers in wild-type mice. With regard to caspase inhibition by zVAD, our data are in line with this report, albeit the TNF α /zVAD-treated mice died at somewhat later time points. Unexpectedly, the additional blockade of necroptosis with either Nec-1 or TAT-crmA did not provide protection, but rather accelerated the time to death (Figure 3). From a clinical point of view, this result is disappointing because Nec-1 or TAT-crmA had been predicted as promising candidates for the treatment of septic shock. We further examined whether this effect was due to the prevention of necroptosis in certain immune cells that could have continued to respond to TNF α by releasing increasing amounts of proinflammatory cytokines, which thereby might have harmed the general organism instead of undergoing PCD, and which might be an effect that is not observed in RIP3-deficient mice because of compensatory mechanisms. Indeed, *ex vivo* analysis of neutrophils taken from intensive care patients concluded that prevention of cell death on cellular level results in earlier death of the individual patient (44). In contrast, the prevention of lymphocyte death improved survival in a murine sepsis model (45). However, depletion of macrophages, NK cells, granulocytes and the administration of TNF α /zVAD/Nec-1 to Balb/c and T-cell deficient mice disproved this hypothesis (Figure S2). It should be mentioned that we cannot formally rule out the possibil-

ity of crmA-mediated interference with other caspases or granzyme B (31,46), but such interaction should not influence the results observed with Nec-1. Importantly, RIP3-deficient mice also are protected from TNF α -mediated shock in the absence of caspase inhibitors (see Figure 2A). Taken together, these results were surprising because the common concept of necroptosis would have favored application of Nec-1 to be in line with genetic RIP-3 deficiency rather than establishing a dichotomy between the two. Therefore, we investigated the consequences of necroptosis inhibition in cerulein-induced pancreatitis which was among the first *in vivo* models that proved the clinical relevance of RIP3-mediated necroptosis (16,25). Interestingly, similar to the TNF α /zVAD-mediated hyperacute shock, the blockade of necroptosis led to the exacerbation of the CIP model (Figure 5). Therefore, two *in vivo* models demonstrate the importance of separating genetic RIP3-deficiency from pharmacologically blocking necroptosis. Inhibition of RIP1 by Nec-1 cannot be equated with the genetic deficiency of RIP3. Apparently, these closely related proteins exhibit different regulatory potentials *in vivo*. Therefore, it will be of interest to see a direct comparison of Nec-1-treatment *versus* RIP3 deficiency in vaccinia virus-infected mice (18) and other *in vivo* models of necroptosis such as the recently published cecal ligation and puncture (CLP) model (47). The latter paper is in line with our data concerning the RIP3-deficient mice, but is in contrast to the results concerning Nec-1 in the TNF-shock model, which might be explained by different concentrations of Nec-1, the different age of the mice or the preparation of the recombinant TNF α used in that study (47).

According to the common concept of TNF α -mediated PCD, complex IIa signals to initiate apoptosis, including the activation of caspase-8. Active caspase-8/FLIP_L heterodimers cleave and inactivate RIP1, thereby preventing necroptotic signaling (10,12). However, recent data from studies on photoreceptors suggests that

necroptosis and apoptosis might not be mutually exclusive (21). Our *in vitro* data concerning HT29 cells and especially FADD-deficient Jurkat cells (see Figure 1) might be interpreted in line with those data. To further clarify this hypothesis we investigated the effect of Nec-1 in the absence of caspase inhibition. We demonstrate the deterioration of TNF α -mediated organ failure by application of Nec-1 at standard and low concentrations of TNF α without the inhibition of caspases. Given that Nec-1 is called a highly specific RIP-1 inhibitor that is even used to define necroptosis (27,48,49), our data suggest direct necroptotic signaling downstream of the TNFR in the absence of caspase inhibition *in vivo*. Importantly, Nec-1 alone, even applied at high plasma concentrations, did not affect survival in the absence of TNF α (data not shown). In TNF α -mediated shock, the comparison of caspase inhibition by zVAD and RIP1 inhibition by Nec-1 resulted in comparable median survival, but the standard deviation in Nec-1-treated animals was lower. One possible explanation for this phenomenon is the strict inhibition of only one protein by Nec-1, whereas zVAD interferes with multiple complexes and delicate signaling conglomerates (50) that may result in a larger standard deviation *in vivo*.

Protection from both TNF α -mediated shock and TNF α /zVAD-mediated hyperacute shock in RIP3-deficient mice as well as the previously described protection in the CIP model suggest that pharmacological inhibition of RIP3 might be of clinical interest. Nec-1 failed to protect in these models, indicating that inhibition of the RIP1/RIP3-pathway must be performed on the level of RIP3 or further downstream.

Results obtained from ischemic myocardium and hypoxic brain injury suggest the pathophysiological presence of both mentioned PCD components (20,21), but other data accumulate for the functional predominance of PN in this setting (51). The principle difference between models of ischemia/reperfusion (I/R) and those of CIP and hyperacute

TNF α -mediated shock is that I/R-models are improved by Nec-1.

CONCLUSION

Taken together, our data outline the importance to separate genetic RIP3-deficiency from Nec-1 application. TAT-crmA provides a powerful tool for the inhibition of intrinsic and extrinsic apoptosis and necroptosis. The fact that Nec-1 and TAT-crmA accelerate disease progression in both CIP and TNF α -mediated shock is disappointing concerning the therapeutic potential of inhibitors of necroptosis. Because various diseases pathophysiologically involve necroptosis, phase 1 clinical trials employing Nec-1 have actually been announced. The need for therapeutic approaches to treat debilitating diseases is obvious. However, aiming to provide the extraordinary potential of Nec-1 or TAT-crmA to patients requires attention, especially in the case of acute inflammation.

ACKNOWLEDGMENTS

We thank Mareike Newsy, Nicole Ahrens, Katarina Stanke, Marina Wirth and Silvia Iversen for their excellent technical support. This work was supported by Werner Jackstädt-Stiftung (A Linkermann) and Fresenius Medical Care Deutschland GmbH (U Kunzendorf and S Krautwald).

DISCLOSURE

The authors declare that they have no competing interests as defined by *Molecular Medicine*, or other interests that might be perceived to influence the results and discussion reported in this paper.

REFERENCES

- Holler N, et al. (2000) Fas triggers an alternative, caspase-8-independent cell death pathway using the kinase RIP as effector molecule. *Nat. Immunol.* 1:489–95.
- Matsumura H, et al. (2000) Necrotic death pathway in Fas receptor signaling. *J. Cell Biol.* 151:1247–56.
- Schulze-Osthoff K, Krammer PH, Droge W. (1994) Divergent signalling via APO-1/Fas and the TNF receptor, two homologous molecules involved in physiological cell death. *EMBO J.* 13:4587–96.
- Vercammen D, et al. (1998) Inhibition of caspases increases the sensitivity of L929 cells to necrosis

- mediated by tumor necrosis factor. *J. Exp. Med.* 187:1477–85.
- Hotchkiss RS, Nicholson DW. (2006) Apoptosis and caspases regulate death and inflammation in sepsis. *Nat. Rev. Immunol.* 6:813–22.
- Hotchkiss RS, Strasser A, McDunn JE, Swanson PE. (2009) Cell death. *N. Engl. J. Med.* 361:1570–83.
- Gerlach B, et al. (2011) Linear ubiquitination prevents inflammation and regulates immune signalling. *Nature.* 471:591–596.
- Haas TL, et al. (2009) Recruitment of the linear ubiquitin chain assembly complex stabilizes the TNF-R1 signaling complex and is required for TNF-mediated gene induction. *Mol. Cell.* 36:831–44.
- Krammer PH, Arnold R, Lavrik IN. (2007) Life and death in peripheral T cells. *Nat. Rev. Immunol.* 7:532–42.
- Vandenabeele P, Galluzzi L, Vanden Berghe T, Kroemer G. (2010) Molecular mechanisms of necroptosis: an ordered cellular explosion. *Nat. Rev. Mol. Cell Biol.* 11:700–14.
- Challa S, Chan FK. (2010) Going up in flames: necrotic cell injury and inflammatory diseases. *Cell Mol. Life Sci.*
- Christofferson DE, Yuan J. (2010) Necroptosis as an alternative form of programmed cell death. *Curr. Opin. Cell Biol.* 22:263–8.
- Declercq W, Vanden Berghe T, Vandenabeele P. (2009) RIP kinases at the crossroads of cell death and survival. *Cell.* 138:229–32.
- Oberst A, et al. (2011) Catalytic activity of the caspase-8-FLIP(L) complex inhibits RIPK3-dependent necrosis. *Nature.* 471:363–7.
- Galluzzi L, et al. (2011) Molecular definitions of cell death subroutines: recommendations of the Nomenclature Committee on Cell Death 2012. *Cell Death. Differ.* 19:107–20.
- He S, et al. (2009) Receptor interacting protein kinase-3 determines cellular necrotic response to TNF-alpha. *Cell* 137:1100–11.
- Vandenabeele P, Vanden Berghe T, Festjens N. (2006) Caspase inhibitors promote alternative cell death pathways. *Sci. STKE.* 2006:e44.
- Cho YS, et al. (2009) Phosphorylation-driven assembly of the RIP1-RIP3 complex regulates programmed necrosis and virus-induced inflammation. *Cell.* 137:1112–23.
- Ch'en IL, et al. (2008) Antigen-mediated T cell expansion regulated by parallel pathways of death. *Proc. Natl. Acad. Sci. U.S.A.* 105:17463–8.
- Trichonas G, et al. (2010) Receptor interacting protein kinases mediate retinal detachment-induced photoreceptor necrosis and compensate for inhibition of apoptosis. *Proc. Natl. Acad. Sci. U.S.A.* 107:21695–700.
- Northington FJ, et al. (2011) Necrostatin decreases oxidative damage, inflammation, and injury after neonatal HI. *J. Cereb. Blood Flow Metab.* 31:178–89.
- Smith CC, et al. (2007) Necrostatin: a potentially novel cardioprotective agent? *Cardiovasc. Drugs Ther.* 21:227–33.

23. Linkermann A *et al.* (2012) Rip1 (receptor-interacting protein kinase 1) mediates necroptosis and contributes to renal ischemia/reperfusion injury. *Kidney Int.* 81:751–61.
24. Kaiser WJ, *et al.* (2011) RIP3 mediates the embryonic lethality of caspase-8-deficient mice. *Nature.* 471:368–72.
25. Zhang DW, *et al.* (2009) RIP3, an energy metabolism regulator that switches TNF-induced cell death from apoptosis to necrosis. *Science.* 325:332–6.
26. Biton S, Ashkenazi A. (2011) NEMO and RIP1 control cell fate in response to extensive DNA damage via TNF- α feedforward signaling. *Cell.* 145:92–103.
27. Degterev A, *et al.* (2008) Identification of RIP1 kinase as a specific cellular target of necrostatins. *Nat. Chem. Biol.* 4:313–21.
28. Cauwels A, Janssen B, Waeytens A, Cuvelier C, Brouckaert P. (2003) Caspase inhibition causes hyperacute tumor necrosis factor-induced shock via oxidative stress and phospholipase A2. *Nat. Immunol.* 4:387–93.
29. Upton JW, Kaiser WJ, Mocarski ES. (2010) Virus inhibition of RIP3-dependent necrosis. *Cell Host. Microbe* 7:302–13.
30. Zhang DW, *et al.* (2011). Multiple death pathways in TNF-treated fibroblasts. *Cell Res.* 2011. 21:368–71.
31. Garcia-Calvo M, *et al.* (1998) Inhibition of human caspases by peptide-based and macromolecular inhibitors. *J. Biol. Chem.* 273:32608–13.
32. Krautwald S, *et al.* (2010) Effective blockage of both the extrinsic and intrinsic pathways of apoptosis in mice by TAT-crmA. *J. Biol. Chem.* 285:19997–20005.
33. Christofferson DE, Yuan J. (2010) Cyclophilin A release as a biomarker of necrotic cell death. *Cell Death. Differ.* 17:1942–3.
34. Newton K, Sun X, Dixit VM. (2004). Kinase RIP3 is dispensable for normal NF- κ Bs, signaling by the B-cell and T-cell receptors, tumor necrosis factor receptor 1, and Toll-like receptors 2 and 4. *Mol. Cell Biol.* 24:1464–9.
35. Chen Y, *et al.* (2010). Dual autonomous mitochondrial cell death pathways are activated by Nix/BNip3L and induce cardiomyopathy. *Proc. Natl. Acad. Sci. U.S.A.* 107:9035–42.
36. Sawai H, Domae N. (2011) Discrimination between primary necrosis and apoptosis by necrostatin-1 in Annexin V-positive/propidium iodide-negative cells. *Biochem. Biophys. Res. Commun.* 411:569–73.
37. Wu YT, *et al.* (2011) zVAD-induced necroptosis in L929 cells depends on autocrine production of TNF α mediated by the PKC-MAPKs-AP-1 pathway. *Cell Death Differ.* 18:26–37.
38. Linkermann A, *et al.* (2011) Renal tubular Fas ligand mediates fratricide in cisplatin-induced acute kidney failure. *Kidney Int.* 79:169–78.
39. Callus BA, Vaux DL. (2007) Caspase inhibitors: viral, cellular and chemical. *Cell Death Differ.* 14:73–8.
40. Gubser C, *et al.* (2007) A new inhibitor of apoptosis from vaccinia virus and eukaryotes. *PLoS Pathog.* 3:e17.
41. Zhou Q, *et al.* (1997) Target protease specificity of the viral serpin CrmA. Analysis of five caspases. *J. Biol. Chem.* 272:7797–800.
42. Krautwald S, Ziegler E, Tiede K, Pust R, Kunzendorf U. (2004) Transduction of the TAT-FLIP fusion protein results in transient resistance to Fas-induced apoptosis in vivo. *J. Biol. Chem.* 279:44005–11.
43. Devalaraja-Narashimha K, Diener AM, Padanilam BJ. (2009) Cyclophilin D gene ablation protects mice from ischemic renal injury. *Am. J. Physiol. Renal Physiol.* 297:F749–59.
44. Cinel I, Opal SM. (2009) Molecular biology of inflammation and sepsis: a primer. *Crit. Care Med.* 37:291–304.
45. Hotchkiss RS, *et al.* (1999) Prevention of lymphocyte cell death in sepsis improves survival in mice. *Proc. Natl. Acad. Sci. U.S.A.* 96:14541–6.
46. Quan LT, Caputo A, Bleackley RC, Pickup DJ, Salvesen GS. (1995) Granzyme B is inhibited by the cowpox virus serpin cytokine response modifier A. *J. Biol. Chem.* 270:10377–9.
47. Duprez L, *et al.* (2011) RIP kinase-dependent necrosis drives lethal systemic inflammatory response syndrome. *Immunity.* 35:908–18.
48. Degterev A, *et al.* (2005) Chemical inhibitor of nonapoptotic cell death with therapeutic potential for ischemic brain injury. *Nat. Chem. Biol.* 1:112–9.
49. Jagtap PG, *et al.* (2007) Structure-activity relationship study of tricyclic necroptosis inhibitors. *J. Med. Chem.* 50:1886–95.
50. Temkin V, Huang Q, Liu H, Osada H, Pope RM. (2006) Inhibition of ADP/ATP exchange in receptor-interacting protein-mediated necrosis. *Mol. Cell Biol.* 26:2215–25.
51. Kung G, Konstantinidis K, Kitsis RN. (2011) Programmed necrosis, not apoptosis, in the heart. *Circ. Res.* 108:1017–1036.